



1 **Flood risk assessment for Indian sub-continental river basins**

2 Urmin Vegad¹, Yadu Pokhrel², and Vimal Mishra^{1,3*}

3

4 ¹Civil Engineering, Indian Institute of Technology (IIT) Gandhinagar

5 ²Civil Engineering, Michigan State University, East Lansing

6 ³Earth Sciences, Indian Institute of Technology (IIT) Gandhinagar

7 *Corresponding author: vmishra@iitgn.ac.in

8 **Abstract**

9 Floods are among India's most frequently occurring natural disasters, which disrupt all aspects of socio-economic
10 well-being. A large population is affected by floods during almost every summer monsoon season in India, leaving
11 its footprint through human mortality, migration, and damage to agriculture and infrastructure. Despite the
12 massive imprints of floods, sub-basin level flood risk assessment is still in its infancy and needs to be improved.
13 Using hydrological and hydrodynamical models, we reconstructed sub-basin level observed floods for the 1901-
14 2020 period. Our modelling framework includes the influence of 51 major reservoirs that affect flow variability
15 and flood inundation. Sub-basins in the Ganga and Brahmaputra River basins witnessed the greatest flood extent
16 during the worst flood in the observational record. Major floods in the sub-basins of the Ganga and Brahmaputra
17 occur during the late summer monsoon season (August-September). Beas, Brahmani, upper Satluj, Upper
18 Godavari, Middle and Lower Krishna, and Vashishti sub-basins are among the most influenced by the dams, while
19 Beas, Brahmani, Ravi, and Lower Satluj are among the most impacted by floods and the presence of dams.
20 Bhagirathi, Gandak, Kosi, lower Brahmaputra, and Ghaghara are India's sub-basins with the highest flood risk.
21 Our findings have implications for flood mitigation in India.

22 **1. Introduction**

23 Flood risk to both natural and human systems is projected to increase due to climate change (IPCC, 2014, 2022).
24 Extreme weather and climate extremes have increased under warming climate, leading to an increased frequency
25 of natural hazards like floods, droughts, heat waves, cyclones, and heavy rains. Hydroclimatic extremes affect
26 humans and infrastructure (Eidsvig et al., 2017; Peduzzi et al., 2009). Due to high vulnerability and lower adaptive
27 capacity, developing countries are often the most impacted by extreme weather events. Further, developing
28 countries usually take longer to recover from the hazards due to low climate resilience. Globally, floods are among
29 the most devastating natural hazards (Ghosh & Kar, 2018). Among all flood types, riverine floods occur most
30 frequently (Kimuli et al., 2021) and often cause substantial damage to agriculture and infrastructure. A
31 considerable fraction of the population and infrastructure are exposed to flooding, which will also increase due to
32 the projected increase in the magnitude and frequency of floods (Winsemius et al., 2018).

33 The increase in flood magnitude due to the warming climate has resulted in considerable economic losses (C. M.
34 R. Mateo et al., 2014; Willner et al., 2018). The total financial loss will likely increase by 17% in the next 20 years
35 due to climate change (Willner et al., 2018). Besides agriculture, floods significantly affect the built environment
36 and transportation infrastructure (Kalantari et al., 2014). For instance, more than 7% of road and railway assets



37 globally are exposed to a 100-year return period flood (Koks et al., 2019). In Asia, about 75% of the population
38 is exposed to riverine floods (Varis et al., 2022). India falls among the top ten most flood-affected countries in
39 Asia and the Pacific (Kimuli et al., 2021). In addition, India is also among the top-ten countries that experienced
40 the highest human mortality due to floods. Considerable population exposure, climate change, and rapid growth
41 and development in flood-prone areas contribute to increased losses from floods.

42 In India, state administration takes decisions to mitigate floods while the central government provides financial
43 aid under severe conditions (Jain et al., 2017). The state authorities develop action plans to minimize flood
44 damage. Therefore, identifying the regions with higher flood risk is essential for planning and mitigation. Flood
45 impacts can be quantified according to the affected population, gross domestic product (GDP), and agricultural
46 practices (Ward et al., 2013). The flood risk assessment framework suggested by the Intergovernmental Panel on
47 Climate Change (IPCC) has been extensively applied at the regional and global scales (Allen et al., 2016; IPCC,
48 2014; Roy et al., 2021). The risk can be quantified as a function of vulnerability, hazard, and exposure (IPCC,
49 2014). To control the risk, reducing vulnerability is considered a short to the mid-term goal (Mishra et al., 2022),
50 while reducing hazards and exposure are long-term goals (Birkmann & Welle, 2015). Flood risk assessment can
51 assist in identifying the regions at high risk due to higher vulnerability, hazard, and exposure, which can be used
52 for developing a framework, methodology, and guidelines for flood mitigation and damage assessment.

53 A flood risk assessment performed on a global scale may not help in identifying the flood risk-prone regions at a
54 country scale due to the coarser spatial resolution (Bernhofen et al., 2022). Due to complex geomorphological
55 characteristics and diverse climatic conditions, India is considered a relatively high flood-risk region (Hochrainer-
56 Stigler et al., 2021). Therefore, estimating flood risk on a finer scale (e.g. sub-basin level) is essential for reliable
57 flood risk assessment. There have been studies on regional or river basin scales (Allen et al., 2016; Ghosh & Kar,
58 2018; Roy et al., 2021); however, those do not provide flood risk at a sub-basin scale in India. In addition, the
59 impact assessment of floods on transport infrastructure (rail and road infrastructure) still needs to be improved in
60 the country (Pathak et al., 2020; Singh et al., 2018). In addition, the role of dams and reservoirs in the flood risk
61 assessment should be addressed (Hirabayashi et al., 2013; Yamazaki et al., 2018). Dams and reservoirs
62 considerably influence streamflow variability and can attenuate flood peaks (Dang et al., 2019; Vu et al., 2022;
63 Zajac et al., 2017). In contrast, dam operations and decisions can also worsen the flood situation in the downstream
64 regions. For instance, recent flooding in Kerala and Chennai was partly attributed to reservoir operations (Mishra
65 & Shah, 2018). India has more than 5300 large dams regulating river flow, affecting ecosystems, natural resources,
66 and livelihoods (Acreman, 2000). Reservoirs impact flow regulation, magnitude, timing, and extent of flooding
67 in the downstream regions. Therefore, flood risk assessment without considering the role of reservoirs can be
68 inappropriate in the basins that are highly affected by the presence of dams.

69 We use the H08 (Hanasaki et al., 2018) global hydrological model combined with the CaMa-Flood (Yamazaki et
70 al., 2011) model for the sub-basin level flood risk assessment in India considering the role of reservoirs. The
71 CaMa-Flood model combined with the H08 model has been used for several river basins globally (Boulangé et
72 al., 2021; C. M. R. Mateo et al., 2013). The CaMa-Flood model performs well in simulating flood dynamics
73 (Chaudhari and Pokhrel, 2022; H. Dang et al., 2022; Gaur & Gaur, 2018; Hirabayashi et al., 2013, 2021; Yamazaki
74 et al., 2018; Yang et al., 2019). The CaMa-Flood model takes runoff as input simulated from any hydrological
75 model and can simulate flood depth and inundation. In India, almost all the major rivers are influenced by



76 reservoirs (Lehner et al., 2011). Therefore, the major scientific questions that we address are: 1) How does the
77 flood risk vary at the sub-basin scale in India for the observed worst floods that occurred during the 1901-2020
78 period? 2) Which are the sub-basins where the presence of reservoirs considerably influences the flood risk? To
79 address these questions, we use long-term observations (1901-2020) from India Meteorological Department
80 (IMD) along with a hydrological modelling framework.

81 **2. Data and Methods**

82 **2.1 Datasets**

83 We used observed gridded precipitation (Pai et al., 2014) and daily maximum and minimum temperatures
84 (Srivastava et al., 2009) from India Meteorological Department (IMD). We obtained gridded daily precipitation
85 at 0.25° from IMD for the 1901-2020 period that was developed using station-based rainfall observations from
86 more than 6900 gauge stations (Pai et al., 2014). The gridded rainfall product has been widely used for
87 hydrological studies (Kushwaha et al., 2021; Shah & Mishra, 2016) and it captures the key features of the summer
88 monsoon variability and orographic rainfall over the western Ghats and foothills of the Himalayas. We obtained
89 daily 1° gridded maximum and minimum temperatures from IMD (Srivastava et al., 2009). The gridded
90 temperature dataset is developed using observations from 395 stations located across India. Bilinear interpolation
91 was used to convert the 1° gridded temperature to 0.25° resolution to make it consistent with the gridded
92 precipitation. For the regions outside India, we obtained observational meteorological datasets (rainfall and
93 temperature) at 0.25 degrees from Princeton University (Sheffield et al., 2006). Gridded datasets from Sheffield
94 et al. (2006) compare well against the IMD observations and have been used in hydrological applications in India
95 (Shah & Mishra, 2016).

96 Observed daily streamflow at gauge stations and reservoir live storage were obtained from India Water Resources
97 Information System (India-WRIS). We considered the influence of 51 major reservoirs located in different river
98 basins to examine the impact of reservoirs on floods using the CaMa-Flood model (Figure S1). The information
99 of dams was obtained from the National Register of Large Dams (NRLD) [Table S1]. We used Global Surface
100 Water (GSW) extent to estimate the flood occurrence at a monthly timescale (Pekel et al., 2016). In addition, we
101 obtained reported flood details from the Emergency Events Database (EM-DAT, <http://www.emdat.be/>) and
102 Dartmouth Flood Observatory (DFO, <http://floodobservatory.colorado.edu/>). EM-DAT is developed by the
103 Centre for Research on the Epidemiology of Disasters (CRED), while the University of Colorado manages DFO.
104 We used population data from Global Human Settlement Layers (GHLS) to estimate flood exposure. Finally, we
105 used roadway and railway network data to assess the impact of floods on the infrastructure.

106 **2.2 H08-CaMa-Flood combined model**

107 We used the H08 (Hanasaki et al., 2018) global hydrological model to simulate hydrological variables. The H08
108 is a distributed global water resources model comprising six sub-models: land surface hydrology, river routing,
109 reservoir operation, crop growth, environmental flow, and water abstraction. The model estimates baseflow using
110 a leaky bucket method, while runoff is calculated based on saturation excess non-linear flow (Hanasaki et al.,
111 2008). The H08 model can be run separately or combined with any hydrodynamic model to perform flow routing.
112 The H08 model uses precipitation, air temperature, short and longwave radiations, wind speed, surface pressure,
113 and specific humidity as input meteorological forcing. Soil parameters for the H08 model were obtained from



114 Harmonized World Soil Database (HWSD). We forced the H08 model with the input meteorological forcing at
115 0.25° spatial and daily temporal resolution. We combined the H08 land surface model with the CaMa-Flood
116 model. The CaMa-Flood model has been previously combined with the H08 model to obtain flood inundation
117 estimates (C. M. Mateo et al., 2014).

118 The CaMa-Flood (version 4.1) is a hydrodynamic model (Yamazaki et al., 2011), which simulates river-floodplain
119 dynamics (Yamazaki et al., 2013). The CaMa-Flood model has been extensively used for better performance in
120 simulating discharge and flood peaks (Zhao et al., 2017). The CaMa-Flood model considers the role of dams and
121 reservoirs for streamflow and flood inundation simulations (Chaudhari & Pokhrel, 2022; C. M. Mateo et al., 2014;
122 Pokhrel et al., 2018). We ran the CaMa-Flood model at a finer spatial resolution (0.1°) using the H08-simulated
123 runoff (0.25°) as input. We calibrated the combined model (H08 and CaMa-Flood) for India's eighteen major river
124 basins for one gauge station, each considering the influence of 51 major dams. The gauge stations were selected
125 in the farthest downstream of the river basin based on the availability of observed streamflow.

126 We manually calibrated the H08 model by adjusting four parameters for each river basin, which include single-
127 layer soil depth, gamma, bulk transfer coefficient, and tau (Hanasaki et al., 2008). We evaluated the model
128 performance using the coefficient of determination (R^2) and Nash-Sutcliffe Efficiency (NSE) for daily streamflow
129 and reservoir live storage. In addition, we compared the simulated and satellite-based observed flood occurrences.
130 The satellite-based flood occurrence is calculated using the Global Surface Water (GSW) dataset (Pekel et al.,
131 2016), available for the 1984-2020 period. We forced the well-calibrated combined (H08 and CaMa-Flood)
132 models with observed meteorological forcing from India Meteorological Department (IMD) at 0.25° spatial
133 resolution to conduct simulations from 1901 to 2020. The H08 model simulated runoff is used in CaMa-Flood to
134 rout flood dynamics at six arc-minutes (0.1 degrees). We generated the flood depth maps for the historical worst
135 flood at the sub-basin level. The worst flood is based on the highest magnitude of river flow observed at the
136 subbasin outlet. The generated flood depths at 6 arc-minutes (0.1°) were further downscaled to 1 arc-minute
137 (~200m) resolution using the downscaling module available within the CaMa-Flood.

138 We used C-ratio (Nilsson et al., 2005; Zajac et al., 2017) to estimate the potential dam effect along a river. The
139 C-ratio is calculated as the ratio of a reservoir's total maximum storage capacity to the mean annual discharge at
140 a selected point along the river downstream (Nilsson et al., 2005; Zajac et al., 2017). We calculated the C-ratio at
141 the outlets of each sub-basins that are influenced by the presence of dams. A lower (less than 0.5) C-ratio indicates
142 that the sub-basin is not considerably affected by the presence of dams. Further, we multiplied the percentage
143 flooded area of each sub-basin with their corresponding C-ratio, which was used to identify the sub-basins that
144 experience considerable flood inundation and are affected by the presence of reservoirs. The identified sub-basins
145 are prone to flooding due to dam operations. Finally, we estimated the exposed rail and road infrastructure affected
146 by floods. The flooded area overlapped over the road and railway network to estimate the network length affected
147 by floods in a sub-basin. We considered the flooded area of the observed worst flood. The subbasins with the
148 highest rail and road infrastructure exposure to floods were identified.

149 **2.3 Risk assessment**

150 We estimated flood risk using hazard, exposure, and vulnerability based on the common framework adopted by
151 the United Nations in the Global Assessment Reports of the United Nations Office for Disaster Risk Reduction



152 (UNISDR, 2011, 2013). A similar framework was used in previous studies for flood risk assessments (C. M. R.
153 Mateo et al., 2014; Tanoue, 2020; Winsemius et al., 2013). We multiplied the normalized values of hazard,
154 exposure, and vulnerability to estimate the risk as:

$$155 \quad \text{Risk} = \text{Vulnerability} * \text{Exposure} * \text{Hazard} \quad \dots \dots (1)$$

156 The flood risk assessment can help identify the hotspots and prioritize climate adaptation (de Moel et al., 2015).
157 Among the three components, vulnerability is a degree of damage to a particular object at flood risk with a
158 specified amount and present on a scale from 0 to 1. We obtained the vulnerability index for each district from
159 the “Climate Vulnerability Assessment for Adaptation Planning in India Using a Common Framework”, a report
160 developed by the Department of Science and Technology
161 (<https://dst.gov.in/sites/default/files/Full%20Report%20%281%29.pdf>). The vulnerability of each district is
162 calculated using 14 indicators, each with equal weights. The indicators capture both sensitivity and adaptive
163 capacity. We estimated the vulnerability index of each sub-basin by taking the spatial mean of the vulnerability
164 of the districts falling into the sub-basins. Exposure is termed as assets and population in a flood-exposed area
165 resulting in flood damage (Marchand et al., 2022). The population dataset is a critical component in performing
166 exposure estimation. The exposure is defined as the fraction of the population exposed to the flood extent (Smith
167 et al., 2019). We completed the flood exposure estimate using the Global Human Settlement Layers (GHSL)
168 population dataset (Joint Research Centre (JRC) et al., 2021), which is available at a resolution of 30 arc-seconds
169 for 1975, 1990, 2000, 2014 and 2015. We used the population data for the year 2015 throughout this study. We
170 rescaled the population data to 6 arc-minutes to make it consistent with the flooded area simulated from the
171 combined model. We estimated the hazard as the exceedance probability of a flooded area exceeding half of the
172 historical maximum flooded area in the last 50 years. We used normalized vulnerability, exposure, and hazard to
173 estimate the risk.

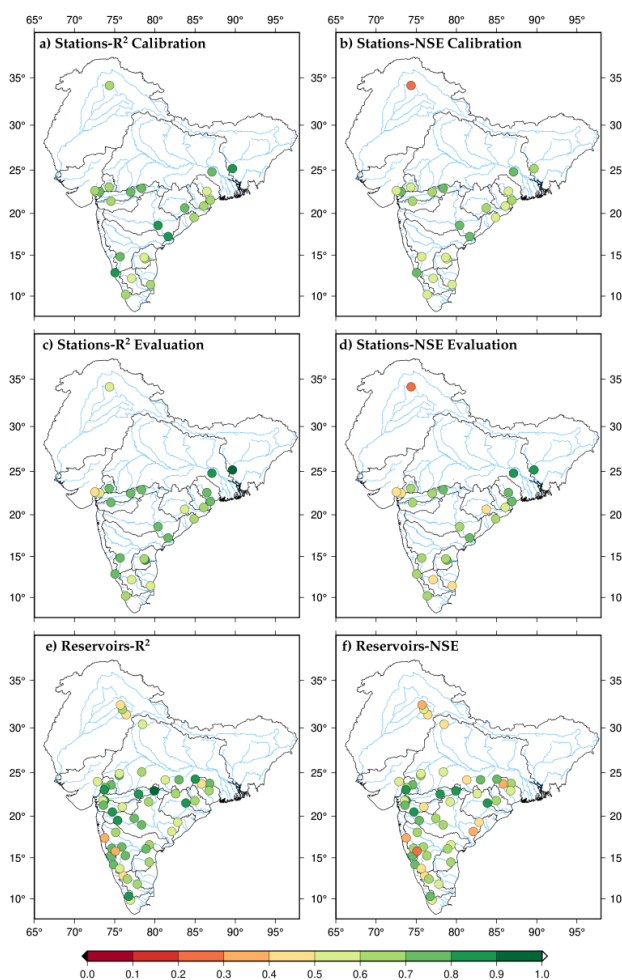
174 3. Results

175 3.1 Calibration and evaluation of hydrological models

176 We calibrated and evaluated the performance of the H08 and CaMa-Flood combined models against the observed
177 daily streamflow (Fig. 1). Due to the unavailability of daily observed streamflow for the three transboundary river
178 basins (Indus, Ganga and Brahmaputra), we used observed monthly streamflow to calibrate the model. In addition,
179 we evaluated the model performance for daily live storage of the 51 reservoirs after the calibration against the
180 observed flow (Fig. 1). The model exhibited good skills ($R^2 > 0.55$ and $NSE > 0.5$) for almost all the river basins
181 except Cauvery, Northeast coast, and Pennar. The model also performed well ($NSE > 0.5$) in simulating daily live
182 storage for the selected reservoirs. In addition, we compared model-simulated, and satellite-based observed flood
183 occurrence for the 1984-2020 period (Fig. 2). The model exhibits satisfactory performance in simulating flood
184 extent against the satellite-based observations. However, the model overestimates the flood extent in the Ganga
185 basin, which can be due to the influence of cloud contamination and dense vegetation cover on satellite-based
186 flood estimates (Chaudhari & Pokhrel, 2022). On the other hand, the model underestimates the flood occurrence
187 in the upstream region of the Brahmaputra River. This could be due to limitations in model parameterization, as
188 observed flow is limited in the transboundary river basins. Despite the good performance against the observed
189 streamflow, the simulated flood extent has a considerable bias, which can be attributed to satellite-based flood

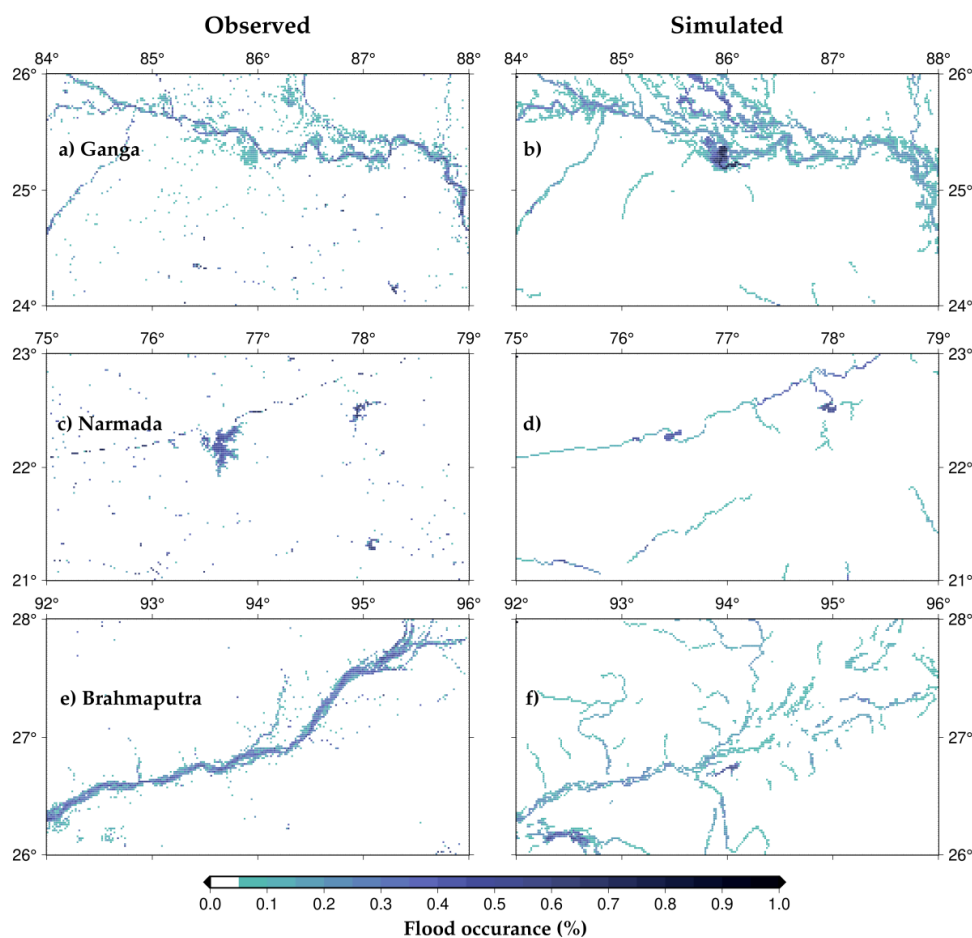


190 extent mapping limitations and the model's ability to capture the flood extent accurately. The model-simulated
191 flood extent shows a good agreement against the reported flood from EM-DAT and DFO databases (Fig. S1). In
192 addition, the simulated flood extent also showed a good agreement with the reported flood in cities in the
193 Brahmaputra and Ganga River basins. Given the limitation in the streamflow and flood extent observations, the
194 hydrological models perform satisfactorily and can be used for the sub-basin level risk assessment.



195

196 **Figure 1: Calibration and evaluation of the combined model for daily river flow and reservoir storage at**
197 **gauge stations and daily live storage of reservoirs**



198

199 **Figure 2: Simulated flood occurrences compared with satellite-based observed flood occurrence for**
200 **different regions in Ganga, Narmada and Brahmaputra River basin.**

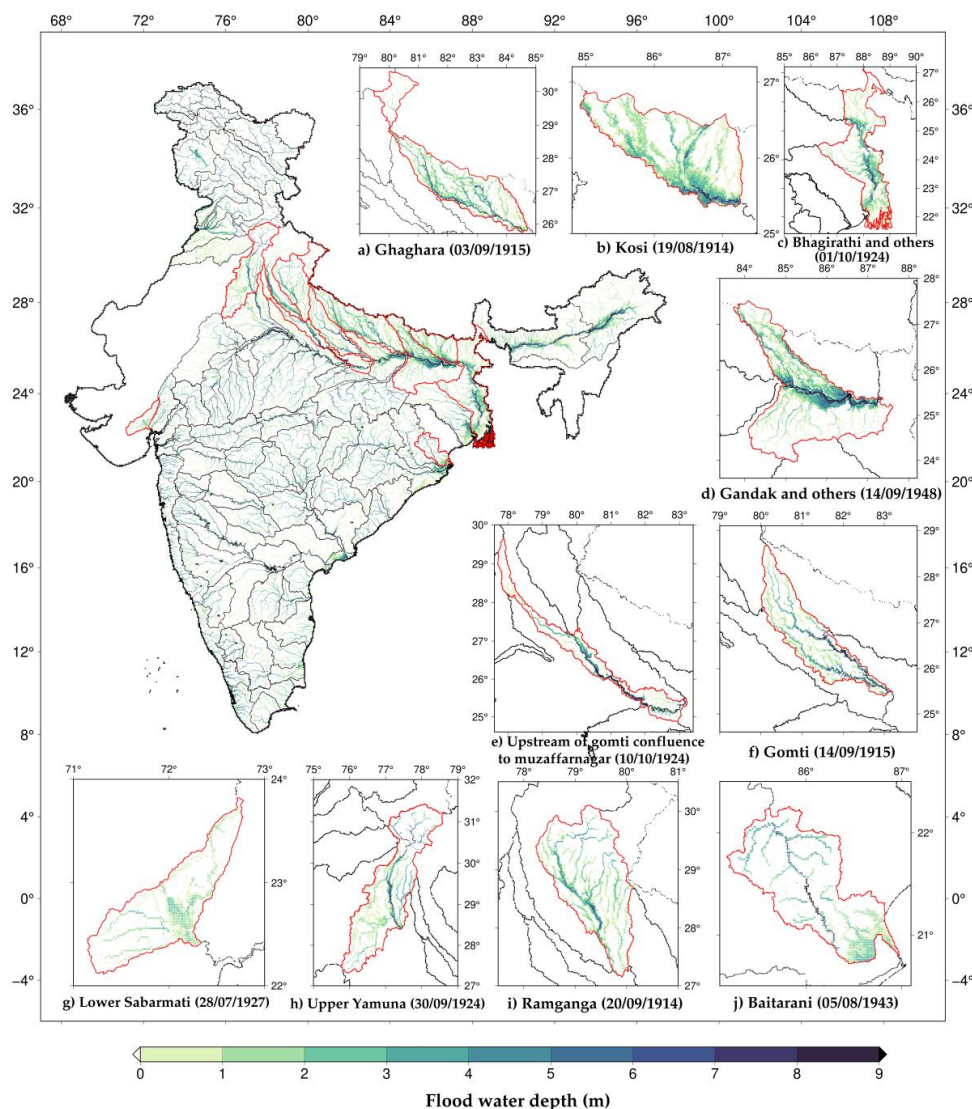
201 3.2 Estimation of the observed flood extent

202 Next, we reconstructed the flood inundation for the observed worst flood for each sub-basin for the 1901-2020
203 period in India. The inundation extent for the worst flood can help us identify the sub-basin with higher flood risk.
204 We estimated flood depth and inundated area for each sub-basin for the worst flood during the last 120 years
205 (Figure 3). In addition, we identified the occurrence of the worst flood at the sub-basin level during the 1901-2020
206 period. We highlighted ten sub-basins that experienced the highest fractional area affected by the worst flood.
207 Sub-basins in the Ganga and Brahmaputra rivers are among the most highly influenced by the worst flood. For
208 instance, Ghaghra, Kosi, Bhagirathi, Gandak, Gomti, lower Sabarmati, upper Yamuna, Ramganga, and Baitarani
209 sub-basins had the highest fractional area affected by the worst flood during 1901-2020 (Fig. 3). The fractional
210 area of sub-basins in the semi-arid western India is less affected compared to those located in the Ganga basin.
211 For example, the lower Sabarmati sub-basin of the Sabarmati River basin is among the sub-basins that are highly



212 influenced by the observed worst flood. We also find that the worst flood in the same year did not affect all the
213 sub-basins within a river basin. For instance, all the highly influenced sub-basins experienced the worst flood in
214 different years in the Ganga basin (Fig. 3). Most of the top flood-affected sub-basins experienced floods during
215 August-September in the summer monsoon season. Overall, the flood extent due to the worst flood is substantially
216 greater in the sub-basins of the Ganga and Brahmaputra river basins compared to other basins in India (Fig. 3).
217 Ganga river basin also has the highest population density among all the basins in the Indian sub-continent, which
218 makes it vulnerable for the flood risk.

219



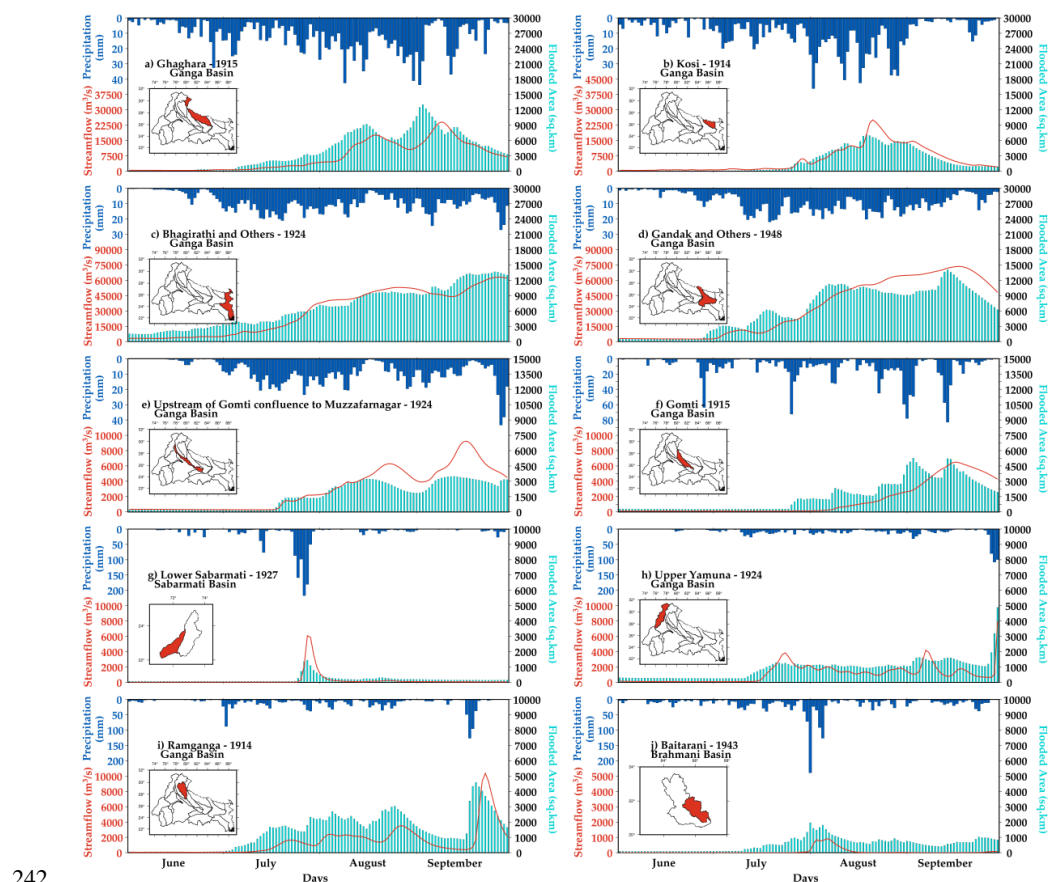
220

221 **Figure 3: Flood depth map for the observed worst flood for each sub-basins, highlighting the sub-basins**
 222 **with maximum flood inundated area (%) (a) Ghaghara – Ganga River basin (b) Kosi – Ganga River basin**
 223 **(c) Bhagirathi and others – Ganga River basin (d) Gandak and others – Ganga River basin (e) Upstream of Gomti**
 224 **confluence to Muzaffarnagar – Ganga River basin (f) Gomti – Ganga River basin (g) Lower**
 225 **Sabarmati – Sabarmati River basin (h) Upper Yamuna – Ganga River basin (i) Ramganga – Ganga River**
 226 **basin (j) Baitarani – Brahmani River basin**

227 Next, we examined the precipitation, streamflow, and flood-affected area (%) for the ten sub-basins that had the
 228 highest fractional flood affected area for the worst flood during 1901-2020 (Fig. 4). As floods mostly occur during
 229 the summer monsoon season in India (Mishra et al., 2022; Nanditha & Mishra, 2021), we examined the temporal



230 variability of precipitation, and streamflow during the monsoon season of the worst flood year. Nanditha and
 231 Mishra (2022) reported that multi-day precipitation is India's most robust driver of floods. Moreover, extreme
 232 precipitation and wet-antecedent conditions trigger floods in India (Nanditha & Mishra, 2022). We find that the
 233 Ghaghara sub-basin of the Ganga river experienced the worst flood in September 1915, affecting more than 10,000
 234 km² area of the sub-basin. A multi-day rainfall in late August and early September (1915) caused the worst flood
 235 in the basin. The Kosi sub-basin of the Ganga river experienced the worst flood in August 2014, which affected
 236 more than 5000 km² of the basin (Fig 4). Similarly, Bhagirathi and other sub-basins in the Ganga river basin were
 237 affected by the worst flood in late September 1924, which inundated more than 12000 km² of the sub-basin.
 238 Similarly, Gandak and Gomti river basins experienced the worst floods in 1948 and 1915, respectively. We find
 239 that most of the sub-basins of the Ganga river basin are prone to large extents of flood inundation. Moreover, the
 240 worst floods in most sub-basins were caused by multi-day precipitation, a prominent driver of floods in the Indian
 241 sub-continental river basins (Fig. 4).

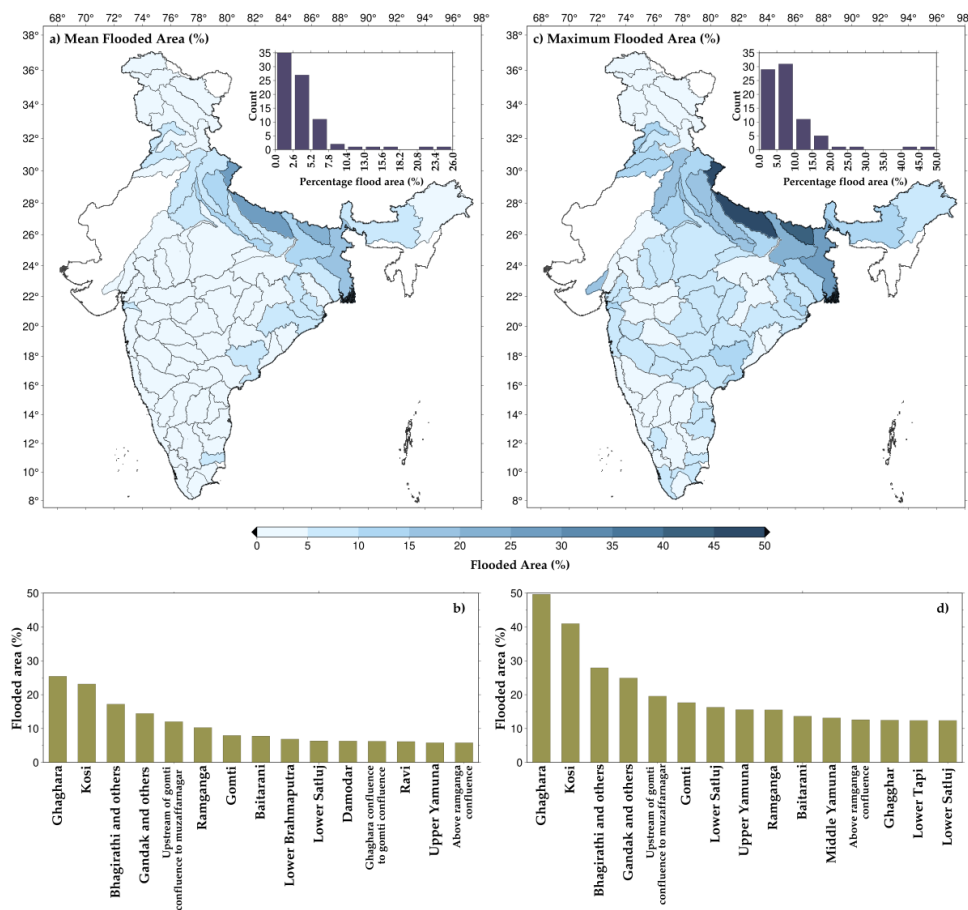


242
 243 **Figure 4: Daily upstream precipitation (mm, blue), the H08 model simulated streamflow (red) at the sub-**
 244 **basin outlet (m³/s), and flooded area (km², green) for the summer monsoon (June-September) period of**
 245 **the corresponding worst flood year. (a) Ghaghara - Ganga River basin (b) Kosi - Ganga River basin (c)**



246 **Bhagirathi and others - Ganga River basin (d) Gandak and others - Ganga River basin (e) Upstream of**
247 **Gomti confluence to Muzaffarnagar - Ganga River basin (f) Gomti - Ganga River basin (g) Lower**
248 **Sabarmati – Sabarmati River basin (h) Upper Yamuna – Ganga River basin (i) Ramganga – Ganga River**
249 **basin (j) Baitarani – Brahmani River basin**

250 To further examine the flood-affected area at the sub-basin level, we estimated the mean annual maximum flooded
251 area (Figure 5a) and historical maximum flooded area using the H08-CaMa flood models (Figure 5b). Most of the
252 highly flooded sub-basins are in the Ganga River basin. While the mean annual maximum flooded area for the
253 top flood-affected sub-basins ranged between 10 to 15%, their maximum flooded area varied between 30 to 40%.
254 Other than sub-basins from the Ganga river basin, Baitarani, lower Tapi, lower Godavari, Brahmani, and lower
255 Mahanadi also showed a considerable mean flooded area during the 1901-1920 period. In the case of the maximum
256 flooded area, Gandak, Kosi, and Ghaghara confluence to Gomti confluence sub-basins exhibited more than 20%
257 flooded area. Sub-basins from the other river basins, such as lower Tapi, lower Narmada, Baitarani, and lower
258 Satluj, are in the top fifteen sub-basins with the highest flooded area. The sub-basins in the Ganga and
259 Brahmaputra rivers are the most flood-affected. Moreover, the Ganga and Brahmaputra rivers experience the
260 highest floods among all the river basins (Mohanty et al., 2020; Mohapatra & Singh, 2003).



261

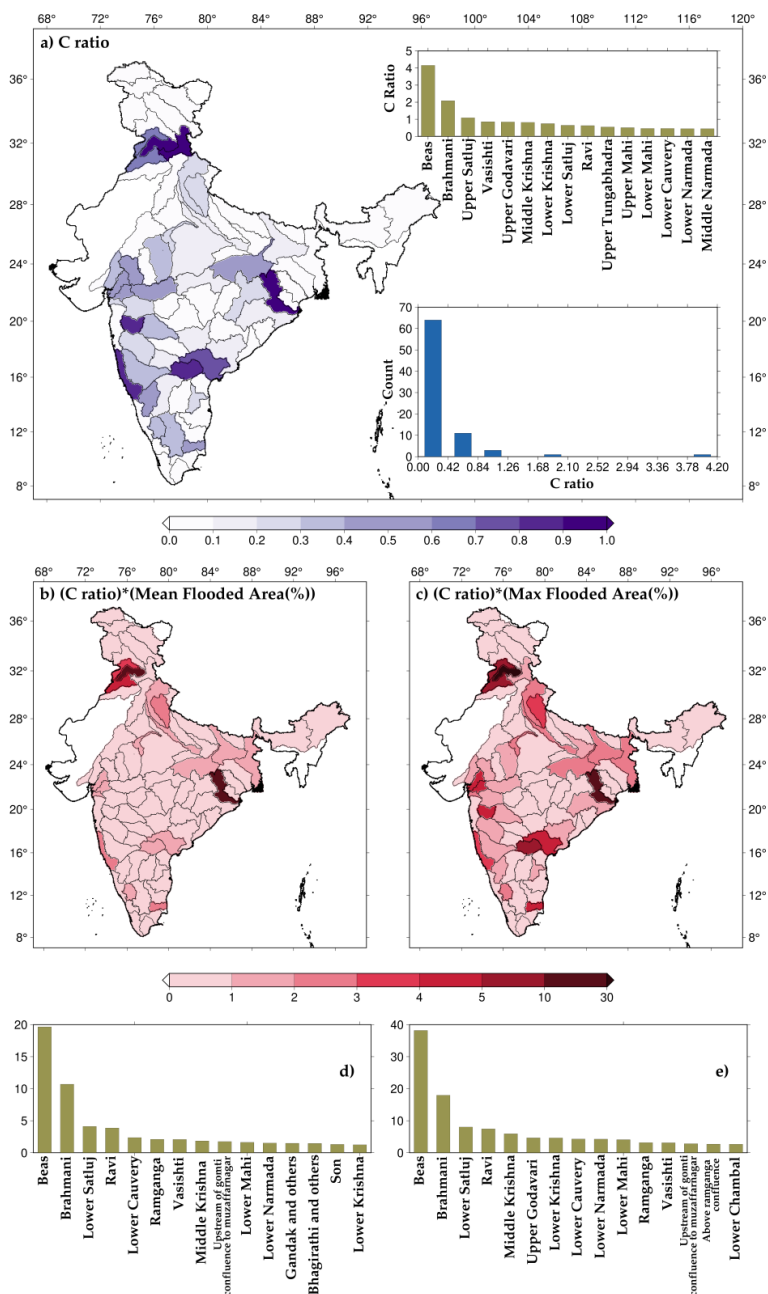
262 **Figure 5: (a) Mean of annual maximum flooded area (percentage) between 1901-2020 and the overall**
 263 **distribution (b) highlighting the top fifteen sub-basin. (c) Historical maximum flooded area (percentage)**
 264 **and the overall distribution (d) highlighting the top fifteen sub-basin.**

265 **3.3 Influence of reservoirs on flood extent**

266 We selected and considered 51 major reservoirs to examine their influence on flood risk based on the availability
 267 of the observed storage data. We estimated C-ratio for each sub-basin considering the river flow at the outlet to
 268 investigate the impact of reservoirs on streamflow. C-ratio can vary between zero to infinity, and higher values
 269 indicate the prominent effect of dams on river flow. We identified sub-basins with a greater influence on dams
 270 based on the C-ratio. We find that Beas, Brahmani, upper Satluj, Upper Godavari, Middle and Lower Krishna,
 271 and Vashishti are among the most influenced by the dams. Beas sub-basin has the highest C-ratio (4.16) among
 272 all the sub-basin in the Indian sub-continent (Figure 6a). Out of the 80 sub-basins, only eleven have C-ratio greater
 273 than 0.5. 64 out of 80 sub-basins have a C-ratio between zero to 0.42 (Figure 6a). We considered only 51 major
 274 reservoirs in our analysis. However, there are several major and minor dams for which observed data is
 275 unavailable. Therefore, the influence of reservoirs based on the C-ratio might need to be considered. However,



276 our analysis indicates that dams in a few sub-basins can significantly alter the river flow and flood risk. For
277 instance, dams effectively alter extreme flow's timing, duration, and frequency (Mittal et al., 2016). C-ratio alone
278 may not effectively capture the influence of dams on floods; therefore, we multiplied the fractional area affected
279 by floods and the c-ratio for each sub-basins. For instance, if a sub-basin is considerably affected by dams and
280 has a large flood extent, the value of the multiplied ratio will be higher. The multiplier ratio can effectively identify
281 the sub-basins with high flood-affected areas and flow regulated by the reservoirs. We find that Beas, Brahmani,
282 Ravi, and Lower Satluj are among the highly influenced by floods and the presence of reservoirs. Overall, the
283 sub-basins with higher C ratio and the highest flood-affected area are across the Indian subcontinent. Central India
284 has sub-basins that are relatively less affected by floods and the presence of dams.



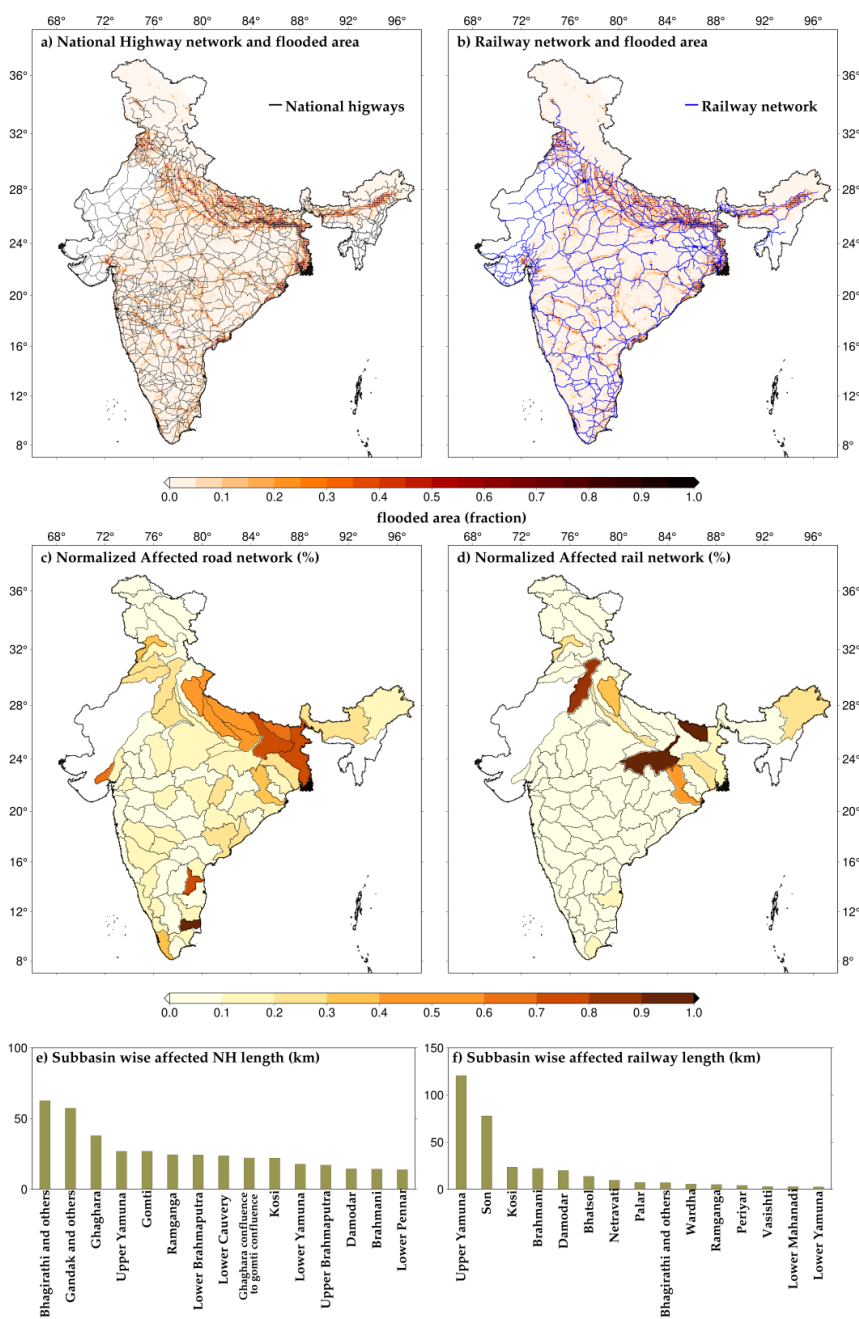
285

286 **Figure 6:** (a) Sub-basin wise C-ratio, top fifteen sub-basins and distribution of sub-basins based on C-ratio
 287 values (b) Mean of annual maximum flooded area (percentage) multiplied with C-ratio (d) highlighting top
 288 15 sub-basins (c) Historical maximum flooded area (percentage) multiplied with C-ratio (e) highlighting
 289 top 15 sub-basins.



290 **3.4 Sub-basin level flood risk assessment**

291 Next, we identified the roads (national highways) and railway exposure to riverine floods for each subbasin.
292 Climate change will adversely affect rail and road networks (Hooper & Chapman, 2012; Padhra, 2022). A
293 considerable length of roads is affected due to surface flooding resulting from high-intensity rain (Koks et al.,
294 2019). Therefore, we examined the impact of floods on rail and road infrastructure in India. We estimated the
295 length of the road and railway network potentially affected by the worst flood that occurred during 1901-2020.
296 We overlapped the road and rail network over the flooded area and estimated the network length exposed to floods
297 (Figure 7a-b). The estimated length for each sub-basin was normalized between zero and one (Figure 7c-d). We
298 find that the road network can be the most affected by the floods in the Gandak, Kosi and Ghaghara confluence
299 to Gomti confluence in the Ganga river basin. On the other hand, a considerable part of the rail network can be
300 affected by floods in Son, Kosi, and Upper Yamuna subbasins. Moreover, in Bhagirathi and Gandak river basins,
301 more than 50 km of road network falls in the flood-prone regions (Figure 7e). There are ten sub-basins in which
302 more than 20 km of road network falls in flood-prone areas of India. Similarly, over 20 km of the rail network is
303 in the flood-affected areas of the six sub-basins (Upper Yamuna, Son, Kosi, Brahmani) [Figure 7f].

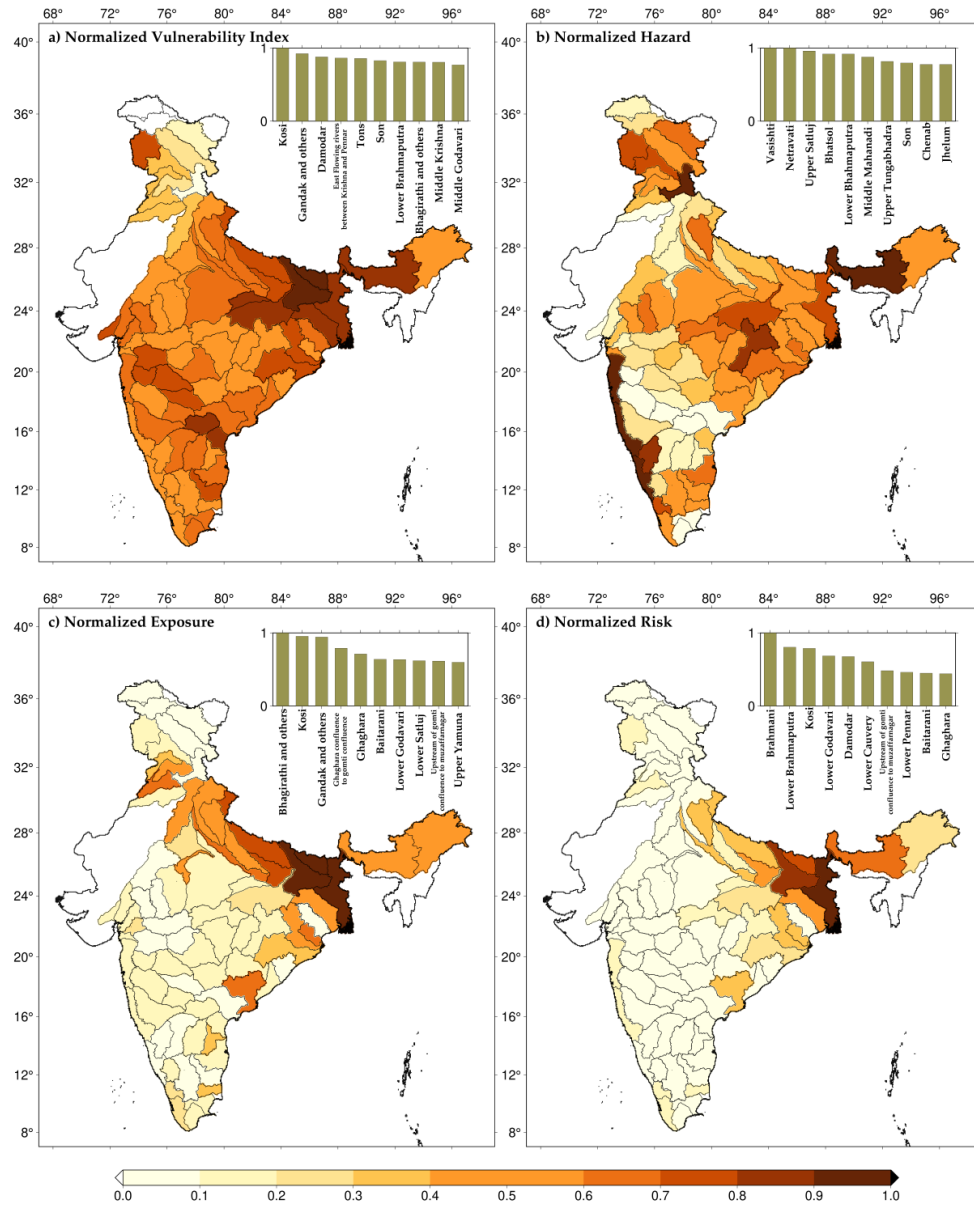


304

305 **Figure 7: Flood impacts on roads and railways infrastructure. (a-b) National Highways network and**
 306 **Railway network overlapped over the flooded area in worst flood cases, (c-d) subbasin wise normalised**
 307 **flood affected road and railway network (percentage), (e-f) top 15 subbasins with most affected national**
 308 **highways and railway length (km).**



309 Finally, we estimated sub-basin level flood risk using normalized vulnerability, hazard, and exposure (Figure 8).
310 Vulnerability for each sub-basin in India was assessed using the national vulnerability assessment data available
311 at the district level. We estimated hazard probability considering 50% of the inundated area for the worst flood as
312 a benchmark. The likelihood of flood inundated areas in a sub-basin exceeding the benchmark was used in the
313 risk assessment. Similarly, we used the worst flood extent and gridded population data to estimate flood exposure.
314 The sub-basins in north-central India have a relatively higher vulnerability calculated using the socio-economic
315 indicators. The vulnerability is relatively lower in north India and the Western Ghats. Kosi, Gandak, and Damodar
316 sub-basins have the highest vulnerability. We find that hazard probability is higher in the sub-basins of
317 Brahmaputra, rivers in the western Ghats, and a few sub-basins of the Indus river basin (Fig. 8b). For instance,
318 upper Satluj, Chenab, and Jhelum sub-basins of the Indus river have higher hazard probability. Other than the
319 Western Ghats, most sub-basins in Peninsular India have relatively lesser hazard probability. Exposure, which
320 represents the fraction of the population affected by flood under the worst flood scenario, is higher in the Indo-
321 Gangetic Plain. Apart from the sub-basins of the Ganga River basin, the lower Brahmaputra, lower Godavari, and
322 Baitarani sub-basin show higher exposure. Therefore, Ganga and Brahmaputra Rivers basins are the highest flood-
323 prone river basins and have high flood exposure. Rentschler et al. (2022) also reported that the highest population
324 exposure due to floods is in Uttar Pradesh, Bihar, and West Bengal, which is part of the Ganga river basin.



325

326 **Figure 8: Sub-basin level (a) Normalized vulnerability index (b) Normalized hazard (c) Normalized**
 327 **exposure (d) Normalized risk. The top 10 sub-basins are highlighted as bars in panels inside the figures.**

328 We estimated the flood risk for each sub-basin, a collective representation of vulnerability, hazard, and
 329 exposure. As expected, the flood risk is higher in the Ganga and Brahmaputra river basins compared to other parts of the
 330 country. The higher flood risk in these basins can be attributed to higher vulnerability, hazard probability, and
 331 exposure. For instance, Bhagirathi, Gandak, Kosi, lower Brahmaputra, and Ghaghra are the sub-basins with the
 332 highest flood risk in India (Fig. 8d). Despite the higher hazard probability in the sub-basins of the Indus and west



333 coast river basins, the overall flood-risk is considerably lower than the sub-basins of the Ganga and Brahmaputra
334 river basins primarily due to less vulnerability and exposure. Our results show that flood risk in some of the sub-
335 basins of the Ganga and Brahmaputra river basins can be reduced by reducing the vulnerability.

336 4. Discussion and conclusions

337 Flood risk mapping is essential for risk reduction and developing mitigation measures. The flood risk will likely
338 increase due to increased hazard probability and exposure (Ali et al., 2019). Hirabayashi et al., 2013) showed that
339 a warmer climate would increase the risk of floods on a global scale. In India also, floods are more likely under
340 warming climate. For instance, Ali et al. (2019) reported that multi-day floods are projected to rise faster than
341 single-day flood events. The projected rise in the flood frequency in India can be attributed to increased extreme
342 precipitation under warming climate (Mukherjee et al., 2018). Observational studies have also concluded that
343 there has been a considerable rise in extreme precipitation in India during the summer monsoon season (Roxy et
344 al., 2017), which is linked to warming climate. While the warming climate is directly linked to the increased
345 frequency of extreme precipitation, its association with riverine floods is not straightforward. For instance,
346 (Nanditha & Mishra, 2021, 2022) reported that multi-day precipitation on the wet antecedent condition is the two
347 most favourable conditions for riverine floods in India.

348 While mapping the flood risk at appropriate spatial resolution is complex and challenging, it is vital for disaster
349 risk reduction. Flood inundation mapping that provides the spatial extent of flooding is crucial as the first
350 responders use it during a flood emergency (Apel et al., 2009). There are several approaches to mapping flood
351 inundation (Teng et al., 2017). We used hydrodynamic modelling to develop long-term flood inundation maps for
352 the Indian sub-basins. Creating higher-resolution flood inundation maps based on hydrodynamic modelling is
353 computationally expensive (Dottori et al., 2016). In addition, higher-resolution flood risk mapping that can be
354 used at the local scale for decision-making requires accurate terrain information and river cross-section datasets
355 that are not available. Given these limitations, our findings provide valuable information based on the long-term
356 record developed using model simulations that can be used for the regional scale policy development for flood
357 mitigation. Cloud cover during the summer monsoon, when most floods occur in India (Nanditha et al., 2022),
358 hinders the utility of satellite data for flood inundation mapping. We calibrated and evaluated our H08-CaMa
359 flood modelling framework using the observed flow, reservoir storage, and satellite-based inundation. However,
360 all these datasets available from the in-situ network or satellites are prone to errors and uncertainty (Di Baldassarre
361 & Montanari, 2009; Stephens et al., 2012; Teng et al., 2017).

362 Notwithstanding the considerable investments and flood-control measures, India has witnessed substantial
363 mortality, human migration, and economic loss. Flood mortality has increased mainly because of increased
364 frequency, not necessarily due to increased flood intensity (Hu et al., 2018). About 3% of the total geographical
365 area of India is affected by floods every year that cause damage to agriculture and infrastructure. The top ten
366 floods that occurred during 1985-2015 caused the mortality of more than 1000 people while more than 35 million
367 people were displaced due to floods between 2000-2004 (Dartmouth Flood Observatory). The recent riverine
368 floods in Uttarakhand and Kerala highlighted the growing flood risk in India, which warrants the need for flood
369 mitigation. The recent flood in August 2022 in Pakistan caused an estimated loss of \$30 billion. Both structural
370 and non-structural measures are required for flood mitigation (Nanditha & Mishra, 2021). Our risk assessment



371 provides policy implications towards reducing vulnerability to reduce the flood risk. Moreover, a sub-basin level
372 ensemble forecast is needed to be used for early flood warnings in the sub-basins with higher flood risk.

373 Based on our findings, the following conclusions can be made:

- 374
- 375 • The coupled hydrological and hydrodynamic modelling framework based on the H08-CaMa Flood model
376 was used to estimate the flood risk assessment in India. The hydrological modelling framework
377 performed well against the observed flow, reservoir storage, and satellite-based flood inundation. The
378 role of 51 major reservoirs was considered in flood risk assessment based on the long-term simulations
for the 1901-2020 period.
 - 379 • The sub-basins in the Ganga and Brahmaputra river basins experienced the most significant flood extent
380 during the worst flood in 1901-2020. Similarly, the mean annual maximum flood extent is higher for the
381 sub-basins in the two major transboundary river basins (e.g., Ganga and Brahmaputra). The worst flood
382 affected different sub-basins on the two main flood-affected river basins in different years. Major floods
383 in the flood-prone sub-basins of the Ganga and Brahmaputra basins occur during the summer monsoon
384 season, especially during the August-September period.
 - 385 • The sub-basins with a more prominent influence of dams based on the C-ratio were identified. Beas,
386 Brahmani, upper Satluj, Upper Godavari, Middle and Lower Krishna, and Vashishti sub-basins are
387 among the most influenced by the dams. Moreover, Beas, Brahmani, Ravi, and Lower Satluj are among
388 the most affected by floods and the presence of reservoirs.
 - 389 • Flood risk is higher in the Ganga and Brahmaputra river basins compared to other parts of the country.
390 The higher flood risk in the two transboundary river basins can be attributed to higher vulnerability,
391 hazard probability, and exposure. Bhagirathi, Gandak, Kosi, lower Brahmaputra, and Ghaghra are India's
392 sub-basins with the highest flood risk.



393 **Data availability:** All the datasets used in this study can be obtained from the corresponding author.

394 **Competing interest:** Authors declare no competing interest.

395 **Author contributions:**

396 **Acknowledgement:** The work was supported by the Monsoon Mission, Ministry of Earth Sciences. The authors
397 acknowledge the data availability from India Meteorological Department (IMD) and India-WRIS. We
398 acknowledge the database availability from EM-DAT: <http://www.emdat.be/>, DFO:
399 <http://floodobservatory.colorado.edu>, population data from GHSL:
400 <https://sedac.ciesin.columbia.edu/data/set/ghsl-population-built-up-estimates-degree-urban-smod>, vulnerability
401 assessment data from DST: <https://dst.gov.in/sites/default/files/Full%20Report%20%281%29.pdf> .

402 **References**

- 403 Acreman, M. (2000). *Managed Flood Releases from Reservoirs: Issues and Guidance*.
404 https://sswm.info/sites/default/files/reference_attachments/ACREMAN%202000%20Managed%20Flood%20Releases%20from%20Reservoirs.pdf
- 406 Ali, H., Modi, P., & Mishra, V. (2019). Increased flood risk in Indian sub-continent under the
407 warming climate. *Weather and Climate Extremes*, 25, 100212.
408 <https://doi.org/10.1016/J.WACE.2019.100212>
- 409 Allen, S. K., Linsbauer, A., Randhawa, S. S., Huggel, C., Rana, P., & Kumari, A. (2016). Glacial lake
410 outburst flood risk in Himachal Pradesh, India: an integrative and anticipatory approach
411 considering current and future threats. *Natural Hazards*, 84(3), 1741–1763.
412 <https://doi.org/10.1007/s11069-016-2511-x>
- 413 Apel, H., Aronica, G. T., Kreibich, H., & Thielen, A. H. (2009). Flood risk analyses - How detailed
414 do we need to be? *Natural Hazards*, 49(1), 79–98. <https://doi.org/10.1007/S11069-008-9277-8/TABLES/5>
- 416 Bernhofen, M. V., Cooper, S., Trigg, M., Mdee, A., Carr, A., Bhawe, A., Solano-Correa, Y. T.,
417 Pencue-Fierro, E. L., Teferi, E., Haile, A. T., Yusop, Z., Alias, N. E., Sa'adi, Z., Bin Ramzan,
418 M. A., Dhanya, C. T., & Shukla, P. (2022). The Role of Global Data Sets for Riverine Flood
419 Risk Management at National Scales. *Water Resources Research*, 58(4).
420 <https://doi.org/10.1029/2021wr031555>
- 421 Birkmann, J., & Welle, T. (2015). Assessing the risk of loss and damage: Exposure, vulnerability and
422 risk to climate-related hazards for different country classifications. *International Journal of*
423 *Global Warming*, 8(2), 191–212. <https://doi.org/10.1504/IJGW.2015.071963>
- 424 Boulange, J., Hanasaki, N., Yamazaki, D., & Pokhrel, Y. (2021). Role of dams in reducing global
425 flood exposure under climate change. *Nature Communications*, 12(1).
426 <https://doi.org/10.1038/s41467-020-20704-0>
- 427 Chaudhari, S., & Pokhrel, Y. (2022). Alteration of River Flow and Flood Dynamics by Existing and
428 Planned Hydropower Dams in the Amazon River Basin. *Water Resources Research*, 58(5).
429 <https://doi.org/10.1029/2021WR030555>



- 430 Dang, H., Pokhrel, Y., Shin, S., Stelly, J., Ahlquist, D., & Du Bui, D. (2022). Hydrologic balance and
431 inundation dynamics of Southeast Asia's largest inland lake altered by hydropower dams in the
432 Mekong River basin. *Science of The Total Environment*, 831, 154833.
433 <https://doi.org/10.1016/J.SCITOTENV.2022.154833>
- 434 Dang, T. D., Chowdhury, A. K., & Galelli, S. (2019). On the representation of water reservoir storage
435 and operations in large-scale hydrological models: implications on model parameterization and
436 climate change impact assessments. *Hydrology and Earth System Sciences Discussions*, 1–34.
437 <https://doi.org/10.5194/hess-2019-334>
- 438 de Moel, H., Jongman, B., Kreibich, H., Merz, B., Penning-Rowsell, E., & Ward, P. J. (2015). Flood
439 risk assessments at different spatial scales. *Mitigation and Adaptation Strategies for Global
440 Change*, 20(6), 865–890. <https://doi.org/10.1007/s11027-015-9654-z>
- 441 Di Baldassarre, G., & Montanari, A. (2009). Uncertainty in river discharge observations: A
442 quantitative analysis. *Hydrology and Earth System Sciences*, 13(6), 913–921.
443 <https://doi.org/10.5194/HESS-13-913-2009>
- 444 Dottori, F., Salamon, P., Bianchi, A., Alfieri, L., Hirpa, F. A., & Feyen, L. (2016). Development and
445 evaluation of a framework for global flood hazard mapping. *Advances in Water Resources*, 94,
446 87–102. <https://doi.org/10.1016/J.ADVWATRES.2016.05.002>
- 447 Eidsvig, U. M. K., Kristensen, K., & Vangelsten, B. V. (2017). Assessing the risk posed by natural
448 hazards to infrastructures. *Natural Hazards and Earth System Sciences*, 17(3), 481–504.
449 <https://doi.org/10.5194/nhess-17-481-2017>
- 450 Gaur, A., & Gaur, A. (2018). *Future Changes in Flood Hazards across Canada under a Changing
451 Climate*. <https://doi.org/10.3390/w10101441>
- 452 Ghosh, A., & Kar, S. K. (2018). Application of analytical hierarchy process (AHP) for flood risk
453 assessment: a case study in Malda district of West Bengal, India. *Natural Hazards*, 94(1), 349–
454 368. <https://doi.org/10.1007/s11069-018-3392-y>
- 455 Hanasaki, N., Kanae, S., Oki, T., Masuda, K., Motoya, K., Shirakawa, N., Shen, Y., & Tanaka, K.
456 (2008). An integrated model for the assessment of global water resources - Part 1: Model
457 description and input meteorological forcing. *Hydrology and Earth System Sciences*, 12(4),
458 1007–1025. <https://doi.org/10.5194/HESS-12-1007-2008>
- 459 Hanasaki, N., Yoshikawa, S., Pokhrel, Y., & Kanae, S. (2018). A global hydrological simulation to
460 specify the sources of water used by humans. *Hydrology and Earth System Sciences*, 22(1), 789–
461 817. <https://doi.org/10.5194/hess-22-789-2018>
- 462 Hirabayashi, Y., Mahendran, R., Koirala, S., Konoshima, L., Yamazaki, D., Watanabe, S., Kim, H., &
463 Kanae, S. (2013). Global flood risk under climate change. *Nature Climate Change*, 3(9), 816–
464 821. <https://doi.org/10.1038/nclimate1911>
- 465 Hirabayashi, Y., Tanoue, M., Sasaki, O., Zhou, X., & Yamazaki, D. (2021). Global exposure to
466 flooding from the new CMIP6 climate model projections. *Scientific Reports*, 0123456789, 1–7.
467 <https://doi.org/10.1038/s41598-021-83279-w>



- 468 Hochrainer-Stigler, S., Schinko, T., Hof, A., & Ward, P. J. (2021). Adaptive risk management
469 strategies for governments under future climate and socioeconomic change: An application to
470 riverine flood risk at the global level. *Environmental Science and Policy*, 125, 10–20.
471 <https://doi.org/10.1016/j.envsci.2021.08.010>
- 472 Hooper, E., & Chapman, L. (2012). The impacts of climate change on national road and rail networks.
473 In *Transport and Sustainability* (Vol. 2, pp. 105–136). Emerald Group Publishing Ltd.
474 [https://doi.org/10.1108/S2044-9941\(2012\)0000002008](https://doi.org/10.1108/S2044-9941(2012)0000002008)
- 475 Hu, P., Zhang, Q., Shi, P., Chen, B., & Fang, J. (2018). Flood-induced mortality across the globe:
476 Spatiotemporal pattern and influencing factors. *Science of The Total Environment*, 643, 171–
477 182. <https://doi.org/10.1016/J.SCITOTENV.2018.06.197>
- 478 IPCC. (2014). *Climate Change 2014: Synthesis Report. Contribution of Working Groups I, II, and III*
479 *to the Fifth Assessment Report of the. Geneva, Switzerland: Intergovernmental Panel on Climate*
480 *Change.*
- 481 IPCC. (2022). *Climate Change 2022: Impacts, Adaptation, and Vulnerability.* Contribution of
482 Working Group II to the Sixth Assessment Report of the Intergovernmental Panel on Climate
483 Change [H.-O. Pörtner, D.C. Roberts, M. Tignor, E.S. Poloczanska, K. Mintenbeck, A. Alegría,
484 M. Craig, S. Langsdorf, S. Löschke, V. Möller, A. Okem, B. Rama (eds.)]. Cambridge
485 University Press. Cambridge University Press, Cambridge, UK and New York, NY, USA, 3056
486 pp., doi:10.1017/9781009325844.
- 487 Jain, G., Singh, C., Coelho, K., & Malladi, T. (2017). *Long-term implications of humanitarian*
488 *responses The case of Chennai.*
489 <http://pubs.iied.org/10840IIEDwww.iied.org@iiedwww.facebook.com/theIIED>
- 490 Joint Research Centre (JRC), European Commission and Center for International Earth Science
491 Information Network (CIESIN), & Columbia University. (2021). *Global Human Settlement*
492 *Layer: Population and Built-Up Estimates, and Degree of Urbanization Settlement Model Grid.*
493 *Palisades, NY: NASA Socioeconomic Data and Applications Center (SEDAC).*
494 <https://doi.org/10.7927/h4154f0w>
- 495 Kalantari, Z., Briel, A., Lyon, S. W., Olofsson, B., & Folkeson, L. (2014). On the utilization of
496 hydrological modelling for road drainage design under climate and land use change. *Science of*
497 *the Total Environment*, 475, 97–103. <https://doi.org/10.1016/J.SCITOTENV.2013.12.114>
- 498 Kimuli, J. B., Di, B., Zhang, R., Wu, S., Li, J., & Yin, W. (2021). A multisource trend analysis of
499 floods in Asia-Pacific 1990–2018: Implications for climate change in sustainable development
500 goals. In *International Journal of Disaster Risk Reduction* (Vol. 59). Elsevier Ltd.
501 <https://doi.org/10.1016/j.ijdr.2021.102237>
- 502 Koks, E. E., Rozenberg, J., Zorn, C., Tariverdi, M., Vousdoukas, M., Fraser, S. A., Hall, J. W., &
503 Hallegatte, S. (2019). A global multi-hazard risk analysis of road and railway infrastructure
504 assets. *Nature Communications*, 10(1). <https://doi.org/10.1038/s41467-019-10442-3>
- 505 Kushwaha, A. P., Tiwari, A. D., Dangar, S., Shah, H., Mahto, S. S., & Mishra, V. (2021). Multimodel
506 assessment of water budget in Indian sub-continental river basins. *Journal of Hydrology*, 603,
507 126977. <https://doi.org/10.1016/J.JHYDROL.2021.126977>



- 508 Lehner, B., Liermann, C. R., Revenga, C., Vörösmarty, C., Fekete, B., Crouzet, P., Döll, P.,
509 Endejan, M., Frenken, K., Magome, J., Nilsson, C., Robertson, J. C., Rödel, R., Sindorf, N., &
510 Wisser, D. (2011). High-resolution mapping of the world's reservoirs and dams for sustainable
511 river-flow management. In *Frontiers in Ecology and the Environment* (Vol. 9, Issue 9, pp. 494–
512 502). <https://doi.org/10.1890/100125>
- 513 Marchand, M., Dahm, R., Buurman, J., Sethurathinam, S., & Sprengers, C. (2022). Flood protection
514 by embankments in the Brahmani–Baitarani river basin, India: a risk-based approach.
515 *International Journal of Water Resources Development*, 38(2), 242–261.
516 <https://doi.org/10.1080/07900627.2021.1899899>
- 517 Mateo, C. M., Hanasaki, N., Komori, D., & Tanaka, K. (2014). Assessing the impacts of reservoir
518 operation to floodplain inundation by combining hydrological, reservoir management, and
519 hydrodynamic models. *AGU Publications*, 7245–7266.
520 <https://doi.org/10.1002/2013WR014845>.Received
- 521 Mateo, C. M. R., Hanasaki, N., Komori, D., Yoshimura, K., Kiguchi, M., Champathong, A.,
522 Yamazaki, D., Sukhannaphan, T., & Oki, T. (2013). A simulation study on modifying
523 reservoir operation rules: Tradeoffs between flood mitigation and water supply. *IAHS-AISH*
524 *Proceedings and Reports*, 362(July), 33–40.
- 525 Mateo, C. M. R., Hanasaki, N., Komori, D., Yoshimura, K., Kiguchi, M., Champathong, A.,
526 Yamazaki, D., Sukhannaphan, T., & Oki, T. (2014). Flood risk and climate change: global
527 and regional perspectives. *Hydrological Sciences Journal*, 59(1), 1–28.
528 <https://doi.org/10.1080/02626667.2013.857411>
- 529 Mishra, V., & Shah, H. L. (2018). Hydroclimatological Perspective of the Kerala Flood of 2018.
530 *Journal of the Geological Society of India*, 92(5), 645–650. <https://doi.org/10.1007/s12594-018-1079-3>
- 532 Mishra, V., Tiwari, A. D., & Kumar, R. (2022). Warming climate and ENSO variability enhance the
533 risk of sequential extremes in India. *One Earth*, 5(11), 1250–1259.
534 <https://doi.org/10.1016/J.ONEEAR.2022.10.013>
- 535 Mittal, N., Bhawe, A. G., Mishra, A., & Singh, R. (2016). Impact of human intervention and climate
536 change on natural flow regime. *Water Resources Management*, 30(2), 685–699.
537 <https://doi.org/10.1007/s11269-015-1185-6>
- 538 Mohanty, M. P., Mudgil, S., & Karmakar, S. (2020). Flood management in India: A focussed review
539 on the current status and future challenges. In *International Journal of Disaster Risk Reduction*
540 (Vol. 49). Elsevier Ltd. <https://doi.org/10.1016/j.ijdr.2020.101660>
- 541 Mohapatra, P. K., & Singh, R. D. (2003). Flood management in India. *Natural Hazards*, 28, 131–143.
542 <https://doi.org/10.1177/0019556120120109>
- 543 Mukherjee, S., Aadhar, S., Stone, D., & Mishra, V. (2018). Increase in extreme precipitation events
544 under anthropogenic warming in India. *Weather and Climate Extremes*, 20, 45–53.
545 <https://doi.org/10.1016/J.WACE.2018.03.005>
- 546 Nanditha, J. S., Kushwaha, A. P., Singh, R., Malik, I., Solanki, H., Singh Chupal, D., Dangar, S.,
547 Shwarup Mahto, S., Mishra, V., Vegad, U., Chupal, D. S., & Mahto, S. S. (2022). The Pakistan



- 548 flood of August 2022: causes and implications. *Authorea Preprints*.
549 <https://doi.org/10.1002/ESSOAR.10512560.1>
- 550 Nanditha, J. S., & Mishra, V. (2021). On the need of ensemble flood forecast in India. *Water Security*,
551 *12*, 100086. <https://doi.org/10.1016/J.WASEC.2021.100086>
- 552 Nanditha, J. S., & Mishra, V. (2022). Multiday Precipitation Is a Prominent Driver of Floods in Indian
553 River Basins. *Water Resources Research*, *58*(7), e2022WR032723.
554 <https://doi.org/10.1029/2022WR032723>
- 555 Nilsson, C., Catherine, *, Reidy, A., Dynesius, M., & Revenga, C. (2005). Fragmentation and Flow
556 Regulation of the World's Large River Systems. In *SCIENCE* (Vol. 308). www.sciencemag.org
- 557 Padhra, A. (2022). Tourism in India and the Impact of Weather and Climate. In *Indian Tourism* (pp.
558 187–197). Emerald Publishing Limited. <https://doi.org/10.1108/978-1-80262-937-820221013>
- 559 Pai, D. S., Sridhar, L., Rajeevan, M., Sreejith, O. P., Satbhai, N. S., & Mukhopadhyay, B. (2014).
560 Development of a new high spatial resolution (0.25° × 0.25°) long period (1901–2010) daily
561 gridded rainfall data set over India and its comparison with existing data sets over the region.
562 *Mausam*, *65*(1), 1–18.
- 563 Pathak, S., Liu, M., Jato-Espino, D., & Zevenbergen, C. (2020). Social, economic and environmental
564 assessment of urban sub-catchment flood risks using a multi-criteria approach: A case study in
565 Mumbai City, India. *Journal of Hydrology*, *591*, 125216.
566 <https://doi.org/10.1016/J.JHYDROL.2020.125216>
- 567 Peduzzi, P., Dao, H., Herold, C., & Mouton, F. (2009). Natural Hazards and Earth System Sciences
568 Assessing global exposure and vulnerability towards natural hazards: the Disaster Risk Index. In
569 *Hazards Earth Syst. Sci* (Vol. 9). www.nat-hazards-earth-syst-sci.net/9/1149/2009/
- 570 Pekel, J. F., Cottam, A., Gorelick, N., & Belward, A. S. (2016). High-resolution mapping of global
571 surface water and its long-term changes. *Nature*, *540*(7633), 418–422.
572 <https://doi.org/10.1038/nature20584>
- 573 Pokhrel, Y., Shin, S., Lin, Z., Yamazaki, D., & Qi, J. (2018). Potential Disruption of Flood Dynamics
574 in the Lower Mekong River Basin Due to Upstream Flow Regulation. *Scientific Reports*, *8*(1).
575 <https://doi.org/10.1038/s41598-018-35823-4>
- 576 Rentschler, J., Salhab, M., & Jafino, B. A. (2022). Flood exposure and poverty in 188 countries.
577 *Nature Communications*, *13*(1). <https://doi.org/10.1038/s41467-022-30727-4>
- 578 Roxy, M. K., Ghosh, S., Pathak, A., Athulya, R., Mujumdar, M., Murtugudde, R., Terray, P., &
579 Rajeevan, M. (2017). A threefold rise in widespread extreme rain events over central India.
580 *Nature Communications*, *8*(1). <https://doi.org/10.1038/s41467-017-00744-9>
- 581 Roy, B., Khan, M. S. M., Saiful Islam, A. K. M., Khan, M. J. U., & Mohammed, K. (2021). Integrated
582 flood risk assessment of the arial khan river under changing climate using ipcc ar5 risk
583 framework. *Journal of Water and Climate Change*, *12*(7), 3421–3447.
584 <https://doi.org/10.2166/wcc.2021.341>



- 585 Shah, H. L., & Mishra, V. (2016). Hydrologic Changes in Indian Subcontinental River Basins (1901–
586 2012). *Journal of Hydrometeorology*, 17(10), 2667–2687. <https://doi.org/10.1175/JHM-D-15-0231.1>
- 588 Sheffield, J., Goteti, G., & Wood, E. F. (2006). *Development of a 50-Year High-Resolution Global*
589 *Dataset of Meteorological Forcings for Land Surface Modeling*.
- 590 Singh, P., Sinha, V. S. P., Vijhani, A., & Pahuja, N. (2018). Vulnerability assessment of urban road
591 network from urban flood. *International Journal of Disaster Risk Reduction*, 28, 237–250.
592 <https://doi.org/10.1016/J.IJDRR.2018.03.017>
- 593 Smith, A., Bates, P. D., Wing, O., Sampson, C., Quinn, N., & Neal, J. (2019). New estimates of flood
594 exposure in developing countries using high-resolution population data. *Nature*
595 *Communications*, 10(1). <https://doi.org/10.1038/s41467-019-09282-y>
- 596 Srivastava, A. K., Rajeevan, M., & Kshirsagar, S. R. (2009). Development of a high resolution daily
597 gridded temperature data set (1969 – 2005) for the Indian region. *Atmospheric Science Letters*,
598 10(October), 249–254. <https://doi.org/10.1002/asl>
- 599 Stephens, E. M., Bates, P. D., Freer, J. E., & Mason, D. C. (2012). The impact of uncertainty in
600 satellite data on the assessment of flood inundation models. *Journal of Hydrology*, 414–415,
601 162–173. <https://doi.org/10.1016/J.JHYDROL.2011.10.040>
- 602 Tanoue, M. (2020). *Future river-flood damage increases under aggressive adaptations*. 1–12.
- 603 Teng, J., Jakeman, A. J., Vaze, J., Croke, B. F. W., Dutta, D., & Kim, S. (2017). Flood inundation
604 modelling: A review of methods, recent advances and uncertainty analysis. *Environmental*
605 *Modelling & Software*, 90, 201–216. <https://doi.org/10.1016/J.ENVSOFT.2017.01.006>
- 606 UNISDR. (2011). *Global Assessment Report on Disaster Risk Reduction 2011, Revealing Risk,*
607 *Redefining Development, United Nations International Strategy*
608 *for Disaster Reduction Secretariat, Geneva, 2011*. https://www.undp.org/publications/2011-global-assessment-report-disaster-risk-reduction?utm_source=EN&utm_medium=GSR&utm_content=US_UNDP_PaidSearch_Brand_English&utm_campaign=CENTRAL&c_src=CENTRAL&c_src2=GSR&gclid=CjwKCAiAqaWdBhAvEiwAGAqlttbTEIs1543d8ZuHyzCatyJutiZP2w2Wp41vZBSiouchJ7PvGpIcUBoCXOYQAvD_BwE
- 614 UNISDR. (2013). *Global Assessment Report on Disaster Risk Reduction 2013, From Shared Risk to*
615 *Shared Value: the Business Case for Disaster Risk Reduction, United Nations International*
616 *Strategy for Disaster Reduction Secretariat, Geneva, 2013*.
617 <https://www.undrr.org/publication/global-assessment-report-disaster-risk-reduction-2013>
- 618 Varis, O., Taka, M., & Tortajada, C. (2022). Global human exposure to urban riverine floods and
619 storms. *River*. <https://doi.org/10.1002/rvr2.1>
- 620 Vu, D. T., Dang, T. D., Galelli, S., & Hossain, F. (2022). Satellite observations reveal 13 years of
621 reservoir filling strategies, operating rules, and hydrological alterations in the Upper Mekong
622 River basin. *Hydrology and Earth System Sciences*, 26(9), 2345–2364.
623 <https://doi.org/10.5194/hess-26-2345-2022>



- 624 Ward, P. J., Jongman, B., Weiland, F. S., Bouwman, A., Van Beek, R., Bierkens, M. F. P., Ligtoet,
625 W., & Winsemius, H. C. (2013). Assessing flood risk at the global scale: Model setup, results,
626 and sensitivity. *Environmental Research Letters*, 8(4). [https://doi.org/10.1088/1748-](https://doi.org/10.1088/1748-9326/8/4/044019)
627 [9326/8/4/044019](https://doi.org/10.1088/1748-9326/8/4/044019)
- 628 Winsemius, H. C., Jongman, B., Veldkamp, T. I. E., Hallegatte, S., Bangalore, M., & Ward, P. J.
629 (2018). Disaster risk, climate change, and poverty: Assessing the global exposure of poor people
630 to floods and droughts. *Environment and Development Economics*, 23(3), 328–348.
631 <https://doi.org/10.1017/S1355770X17000444>
- 632 Winsemius, H. C., van Beek, L. P. H., Jongman, B., Ward, P. J., & Bouwman, A. (2013). A
633 framework for global river flood risk assessments. *Hydrology and Earth System Sciences*, 17(5),
634 1871–1892. <https://doi.org/10.5194/hess-17-1871-2013>
- 635 Yamazaki, D., De Almeida, G. A. M., & Bates, P. D. (2013). Improving computational efficiency in
636 global river models by implementing the local inertial flow equation and a vector-based river
637 network map. *Water Resources Research*, 49(11), 7221–7235.
638 <https://doi.org/10.1002/wrcr.20552>
- 639 Yamazaki, D., Kanae, S., Kim, H., & Oki, T. (2011). A physically based description of floodplain
640 inundation dynamics in a global river routing model. 47(February), 1–21.
641 <https://doi.org/10.1029/2010WR009726>
- 642 Yamazaki, D., Watanabe, S., & Hirabayashi, Y. (2018). Global Flood Risk Modeling and Projections
643 of Climate Change Impacts. *Global Flood Hazard: Applications in Modeling, Mapping, and*
644 *Forecasting*, 233, 185–203. <http://cmip-pcmdi.llnl.gov/>
- 645 Yang, T., Sun, F., Gentine, P., Liu, W., Wang, H., Yin, J., Du, M., & Liu, C. (2019). Evaluation and
646 machine learning improvement of global hydrological model-based flood simulations.
647 *Environmental Research Letters*, 14(11). <https://doi.org/10.1088/1748-9326/ab4d5e>
- 648 Zajac, Z., Revilla-Romero, B., Salamon, P., Burek, P., Hirpa, F., & Beck, H. (2017). The impact of
649 lake and reservoir parameterization on global streamflow simulation. *Journal of Hydrology*, 548,
650 552–568. <https://doi.org/10.1016/j.jhydrol.2017.03.022>
- 651 Zhao, F., Veldkamp, T. I. E., Frieler, K., Schewe, J., Ostberg, S., Willner, S., Schauburger, B.,
652 Gosling, S. N., Schmied, H. M., Portmann, F. T., Leng, G., Huang, M., Liu, X., Tang, Q.,
653 Hanasaki, N., Biemans, H., Gerten, D., Satoh, Y., Pokhrel, Y., ... Yamazaki, D. (2017). The
654 critical role of the routing scheme in simulating peak river discharge in global hydrological
655 models. *Environmental Research Letters*, 12(7). <https://doi.org/10.1088/1748-9326/aa7250>
- 656